

学位申請論文

主論文題目

Magnetic Circular Dichroism of Spin-Forbidden Transitions
in Fe³⁺ High-Spin System

(高スピンの鉄化合物におけるスピンの禁制遷移の磁気円二色性)

学位申請者

加藤 肇

主 論 文

THE JOURNAL OF CHEMICAL PHYSICS

A RESEARCH JOURNAL DEVOTED TO THE BORDER-LINE FIELD
OF PHYSICS AND CHEMISTRY PUBLISHED BY THE

AMERICAN INSTITUTE OF PHYSICS

理

167 西

J. W. STOUT
EDITOR

DEPARTMENT OF CHEMISTRY
UNIVERSITY OF CHICAGO
CHICAGO, ILLINOIS 60637

12 April 1972

File No.: 245A2

Authors: Hajime Kato

Title: Magnetic Circular Dichroism of Spin-Forbidden Transitions
in Fe^{3+} High-Spin System

Tentative Issue: 15 July 1972

Category: Article

Dr. Hajime Kato
Department of Chemistry
Kobe University
Nada-ku, Kobe, Japan

Dear Dr. Kato:

The above manuscript has been accepted for publication in the Journal of Chemical Physics and is being forwarded to the American Institute of Physics publication office. Please read the enclosed material and notice that a completed copy of the Publication Charge Certification form must be received by the Director of Publications, American Institute of Physics before your manuscript will be processed.

An estimate of the approximate number of pages, N , may be obtained by the formula

$$N \approx 0.3 P + 0.25 F.$$

P is the number of full typewritten pages, including title, by-line, abstract, text, tables, and references. F is the number of figures.

Sincerely yours,

J. W. Stout

JWS:mz
enclosures

Magnetic Circular Dichroism of Spin-Forbidden
Transitions in Fe³⁺ High-Spin System

Hajime Katô

Department of Chemistry, Faculty of Science,
Kobe University, Nada-ku, Kobe, Japan

The magnetic circular dichroism (MCD) of the aqueous solution of potassium tris(oxalato)ferrate(III) is measured at room temperature over the region 400 nm~750 nm. The MCD of the spin-forbidden d-d transitions of high spin iron(III) complexes is analyzed on the basis of ligand field theory. The electric dipole transition moments are calculated for two cases where d-d transitions are allowed by odd crystal field and by odd vibrations. The MCD analyses prove that the vibrations of T_{1u} mode are effective in promoting transition ${}^6A_{1g} \rightarrow {}^4T_{2g}(1)$. Comparison of the theoretically derived Faraday parameters with the observed MCD shows that the band at 640 nm is the transition ${}^6A_{1g} \rightarrow {}^4T_{2g}(1)$ and that the band at 445 nm is composed of two transitions: transition ${}^6A_{1g} \rightarrow {}^4A_{1g}$ at higher energy region and transition ${}^6A_{1g} \rightarrow {}^4E_g(1)$ at lower energy region. The huge MCD of these transitions arises mainly from the C term, which have its origin in the spin-degeneracy of the ground state.

I. INTRODUCTION

The polarized absorption spectrum of the trigonally distorted compound $\text{NaMgFe}(\text{ox})_3$ at 77°K was reported by Piper and Carlin¹, and the polarized spectrum of $(\text{NH}_4)_3\text{Fe}(\text{mal})_3$ was reported by Hatfield². More recently Kolt and Dingle³ have reported the spectra of $\text{Fe}(\text{urea})_6(\text{ClO}_4)_3$ and $\text{NaMgFe}(\text{ox})_3$ at 20°K , and concluded that while the absorption spectra of high spin iron(III) complexes might be assigned on energy grounds, no detail information as to the nature of the d-d transitions might be obtained from polarization data.

Recent magnetic circular dichroism (MCD) studies⁴⁻⁶ have demonstrated the utility of MCD spectroscopy in characterizing the symmetry of transitions and clarifying spectroscopic assignments. In case where the ground state is spin-degenerate but orbitally nondegenerate, the MCD of spin-forbidden transition shows huge effects⁷. In this paper the MCD spectra of the aqueous solution of potassium trismalonatoferrate(III) are presented and an assignment of the spectrum is intended. Our purpose in this work is also to estimate the MCD parameters and attack the question what is the main source of the MCD of ferric ion.

The molar ellipticity ($[\theta]_M$) per unit magnetic field for a transition $a \rightarrow j$ of molecules oriented at random in a magnetic field H_s along the direction of propagation of the light are given by^{7,8}

$$[\theta(a \rightarrow j)]_M = - \frac{2hN}{hc} \{ A(a \rightarrow j) r_1 + [B(a \rightarrow j) + C(a \rightarrow j)/kT] r_2 \}, \quad (1)$$

where

$$A(a \rightarrow j) = (2g_a)^{-1} \sum \langle k | j \rangle \langle j | a \rangle \cdot \text{Im} \{ \langle a | m | j \rangle \langle j | m | a \rangle \}, \quad (2)$$

$$B(a \rightarrow j) = (g_a)^{-1} \sum \text{Im} \left\{ \sum_{k \neq a} \frac{\langle k | j \rangle \langle j | a \rangle}{h\nu_{ka}} \cdot \langle a | m | j \rangle \langle j | m | k \rangle \right. \\ \left. + \sum_{k \neq j} \frac{\langle j | m | k \rangle}{h\nu_{kj}} \cdot \langle a | m | j \rangle \langle k | m | a \rangle \right\}, \quad (3)$$

$$C(a \rightarrow j) = (2g_a)^{-1} \sum \langle a | m | a \rangle \cdot \text{Im} \{ \langle a | m | j \rangle \langle j | m | a \rangle \}, \quad (4)$$

$$r_1 = \frac{4\nu_{ja} \nu^3 (\nu_{ja}^2 - \nu^2) \Gamma_{ja}}{h [(\nu_{ja}^2 - \nu^2)^2 + \nu^2 \Gamma_{ja}^2]}, \quad r_2 = \frac{\nu^3 \Gamma_a}{(\nu_{ja}^2 - \nu^2)^2 + \nu^2 \Gamma_{ja}^2}, \quad (5)$$

$\underline{m} = \sum_i e_i \underline{r}_i$, $\chi = \sum_i -\beta(\nu_i + 2s_i)$, $h\nu_{ja} = E_j - E_a$ is the energy difference between the states j and a , N is Avogadro's number, g_a is the degeneracy of ground state a , and Γ_{ja} is the band width of the $a \rightarrow j$ transition. The summations in Eqs.(2)~(4) are over all transitions degenerate with $a \rightarrow j$.

A powerful technique for extracting quantitative values for A , B , and C from the experimental data is the method of moments^{9,10}. The zeroth moment of the MCD satisfies the relation:

$$\int_{\text{band}} ([\theta]_M / \nu) d\nu = -33.53 (B + C/kT), \quad (6)$$

where $(B + C/kT)$ is expressed in square Debye· β per cm^{-1}

($\beta = \text{Bohr magneton}$), and $[\theta]_M$ is expressed in the conventional units of natural optical activity per unit magnetic field.

II. EXPERIMENTAL

The visible and ultraviolet absorption and MCD spectra of the trismalonatoferrate(III) ion, $\text{Fe}(\text{C}_3\text{H}_2\text{O}_4)_3^{3-}$, were measured in pure water solution of potassium tris(malonato)ferrate(III) at room temperature ($27 \pm 1^\circ\text{C}$). This complex was prepared by the method given in the literature¹¹. The MCD of a solution was measured first with solute and then without; the latter trace provided the MCD baseline. The absorption spectrum and MCD of $\text{Fe}(\text{C}_3\text{H}_2\text{O}_4)_3^{3-}$ are shown in Fig.1, and the MCD baseline is also recorded in it.

Fig.1

The absorption and MCD spectra were recorded using a JASCO automatic recording spectrometer model J-10. A permanent magnet with an 8 mm axial hole and a 13 mm pole gap was placed in the sample compartment. The magnetic field was about 4500 gauss. The sample was poured into a quartz cell with 10 mm optical path. Reproducible MCD spectra were obtained at the most sensitive scale (1×10^4 Absorbance/cm). The MCD was expressed as molar ellipticity $[\Theta]_M$ in degree decimeter⁻¹ mole⁻¹ gauss⁻¹. An aqueous solution of d-10-camphor-sulfonic acid (1 mg/ml) was chosen as the reference sample ($A_{290\text{nm}} = 0.00947$ per cm).

III. CALCULATION OF PARADAY PARAMETER

To evaluate the Paraday parameter Δ , B , and C given by Eq.(2)~(4), we must determine the excited state wavefunctions and excitation energies. It is well established that the ligand field theory gives the correct description of the lowlying excited states of the octahedral ions^{12,13}. Piper and Carlin¹ adjusted the parameters Dq , B , and C assuming an octahedral field for $Fe(\underline{ox})_3^{3-}$ so that the calculated energies of the transitions ${}^6A_{1g} \rightarrow {}^4A_{1g}$, ${}^6A_{1g} \rightarrow {}^4T_{1g}$, and ${}^6A_{1g} \rightarrow {}^4T_{2g}$ (of 4G) agree with the experimental ones, and obtained $Dq=1522$, $B=609$, and $C=3283 \text{ cm}^{-1}$. Hatfield² obtained $Dq=1419$, $B=609$, and $C=3135 \text{ cm}^{-1}$ for $Fe(C_3H_2O_4)_3^{3-}$ in the same way, and showed that the observed higher energy band agrees well with the energy of the ${}^6A_{1g} \rightarrow {}^4T_{2g}$ (4D) transition predicted using the experimental parameters. For simplicity, we shall adopt the parameters $Dq=1500$, $B=600$, and $C=3200 \text{ cm}^{-1}$, and set up the matrices of Tanabe and Sugano¹³ for the 4E_g , ${}^4T_{1g}$, and ${}^4T_{2g}$ states in terms of these parameters. By solving the secular equations of the energy matrices, we can determine the excitation energies and state wavefunctions.

The results obtained are listed in Table I. In the calculation of $B(a \rightarrow j)$ in Eq.(3), we neglect the mixing of the other higher energy states. This approximation is reasonable, since the main contribution of Zeeman effect to the lower energy $d-d$ transitions comes from the mixing of near energy bands.

Table I

To complete the quantitative prediction of Faraday parameters, it is necessary to evaluate the magnetic dipole moments and electric dipole moments. The magnetic dipole matrix elements can easily be expressed in terms of one-electron matrix elements¹², and the one-electron matrix elements of \hat{Q} are well known.

Electric dipole transitions are forbidden between the states of d^n electron configuration, since the states belong to the same parity. However, in the crystal in which absorption centers have no center of symmetry, this selection rule is slightly released both by odd crystal field and by odd vibrations. The latter exist always in any crystal even in which absorption centers have a center of symmetry.

In $\text{Fe}(\text{ox})_3^{3-}$, the metal ion is on a site of D_3 symmetry¹³. The splitting of the ${}^4A_{1g}$ and 4E_g levels as a result of the lower symmetry associated with $\text{Fe}(\text{C}_2\text{H}_2\text{O}_4)_3^{3-}$ is reported to be less than that observed for $\text{Fe}(\text{ox})_3^{3-}$ ¹⁴. However, the symmetry of the $\text{Fe}(\text{C}_2\text{H}_2\text{O}_4)_3^{3-}$ ion is also D_3 . Therefore, it is necessary to know the contribution of each cause: odd crystal field and odd vibrations. In the below, we shall first rest our attention to the electric dipole transitions allowed by odd vibrations, and next consider the electric dipole transitions caused by small odd crystal field.

A. Electric Dipole Transition Caused by Odd Vibrations

We assume here that the crystal field is due to the

six point dipoles of moment μ vibrating about the equilibrium positions $(\pm R, 0, 0)$, $(0, \pm R, 0)$, and $(0, 0, \pm R)$ without changing their directions given by $(\pm 1, 0, 0)$, $(0, \pm 1, 0)$, and $(0, 0, \pm 1)$, respectively. The calculation of electric dipole transition moments is made on the basis of the theory by Koide and Pryce (referred to KP in the following). Bearing in mind that the ground state ${}^6A_{1g}$ is the only sextet obtained from $3d^5$ configuration and that the ground state ${}^6A_{1g}$ couple only with ${}^4T_{1g}$ states through the spin-orbit interaction

$$H_{so} = \zeta \sum_i \mathbf{l}_i \cdot \mathbf{s}_i, \text{ we get}$$

$$\langle {}^4f: n' | \mathbf{m} | {}^6A_{1g}: n \rangle = - \sum_{k=1,2,3} \frac{\langle {}^4f: n' | \mathbf{m} | {}^4T_{1g}(k): n \rangle \langle {}^4T_{1g}(k): n | H_{so} | {}^6A_{1g}: n \rangle}{E_{{}^4T_{1g}(k)} - E_{{}^6A_{1g}}}$$

The spin-orbit interaction parameter is approximated to be 400 cm^{-1} . Using closure properties of the eigenfunctions, we approximate the electric dipole transition moment, which is allowed by odd vibration H_v , between initial and final states as

$$\langle {}^4i: n | \mathbf{m} | {}^4f: n' \rangle = - \frac{2}{5E} \langle {}^4i: n | \mathbf{m} | H_v | {}^4f: n' \rangle \quad (8)$$

As in KP we shall assume that the molecule is initially in the vibrationally lowest energy state $n=0$, and that the final vibrational state is the one in which only one vibrational quantum number is excited, i.e. $n'=1$. Then,

$$\langle {}^4i: 0 | \mathbf{m} | {}^4f: n'_{jw}=1 \rangle = - \frac{2}{5E} \left(\frac{\hbar}{2M \omega_{jw}} \right)^{1/2} \langle {}^4i | \sum_k \mathbf{m}_k u_{jw}(x_k) | {}^4f \rangle \quad (9)$$

The matrix elements $\langle {}^4i | \sum_k \mathbf{m}_k u_{jw}(x_k) | {}^4f \rangle$ can be reduced to

the sum of one-electron integrals, which are given as a function of $e\langle r^2 \rangle / R^4$, $e\langle r^4 \rangle / R^6$, and $e\langle r^6 \rangle / R^8$ (where $\langle \rangle$ represents the average with respect to the radial part of $3d$ function).

The numerical value of $e\langle r^4 \rangle / R^6$ is approximately evaluated by using the relationship, $10Dq = \frac{22}{3} \frac{e\langle r^4 \rangle}{R^6}$, which is the magnitude of the splitting of the $3d$ -level in a cubic field. The values of $\langle r^2 \rangle$, $\langle r^4 \rangle$ and $\langle r^6 \rangle$ are calculated by using an analytical SCF wavefunction for Fe atom obtained by Clementi¹⁶. The values are $\langle r^2 \rangle_{Fe} = 1.538a_0^2$, $\langle r^4 \rangle_{Fe} = 5.852a_0^4$, and $\langle r^6 \rangle_{Fe} = 50.167a_0^6$. The values of $e\langle r^2 \rangle / R^4$ and $e\langle r^6 \rangle / R^8$ are obtained by using the value of $e\langle r^4 \rangle / R^6$ and the calculated ratios $\langle r^2 \rangle / \langle r^4 \rangle$ and $\langle r^6 \rangle / \langle r^4 \rangle$, and assuming R to be $4a_0$. The mean energy difference δE is assumed to be 10^5 cm^{-1} . The mass M of a ligand is approximated by that of oxygen atom. The unknown infrared frequencies of the normal mode $T_{1u}(\nu_3)$, $T_{1u}(\nu_4)$, and $T_{2u}(\nu_5)$ are assumed to be 200 cm^{-1} , 400 cm^{-1} , and 100 cm^{-1} , respectively¹⁷. Then, we can calculate the electric dipole transition moments, and the oscillator strengths of the lower energy transitions are shown in Table II.

Table II

We can now calculate the Faraday parameters. In the limit of zero spin-orbit coupling, \underline{A} , \underline{B} , and \underline{C} are independent of spin and only orbital degeneracy contributes to \underline{A} and \underline{C} terms. However, the ground state of Fe^{3+} ion is ${}^6A_{1g}$ and the spin-forbidden transitions can be allowed by spin-orbit

coupling of the ground state ${}^6A_{1g}$ with the excited states ${}^4T_{1g}$. The spin-orbit coupling mixes states of different total spin, and the following relations are satisfied;

$$\text{Im}\{ \langle {}^6A_{1g}(M_S) | \underline{C} | {}^4T_{1g}(M_S') \rangle \sum_{\underline{m}} \langle {}^4T_{1g}(M_S') | \underline{C} | {}^6A_{1g}(M_S) \rangle \}$$

$$= - \text{Im}\{ \langle {}^6A_{1g}(-M_S) | \underline{C} | {}^4T_{1g}(-M_S') \rangle \sum_{\underline{m}} \langle {}^4T_{1g}(-M_S') | \underline{C} | {}^6A_{1g}(-M_S) \rangle \},$$

where M_S and M_S' are the eigenvalues of spin angular moment s_z . The \underline{C} and \underline{A} terms of the split components of the transition no longer cancel and no longer independent of spin. Therefore, all the spin-forbidden transitions of Fe^{3+} high-spin systems can exhibit \underline{A} and \underline{C} terms independently of orbital degeneracy. The resultant MCD of spin-dependent \underline{A} and \underline{C} terms shows usual Faraday \underline{A} and \underline{C} term lineshapes, respectively. The numerical parameters obtained for transitions ${}^6A_{1g} \rightarrow {}^4A_{1g}$, ${}^6A_{1g} \rightarrow {}^4E_g(1)$, and ${}^6A_{1g} \rightarrow {}^4T_{2g}(1)$ are given in Table III. In the evaluation of the 1-st term in Eq.(3), we have used the Eq.(7) where \underline{m} is replaced by \underline{m}' .

Table III

B. Electric Dipole Transition Caused by Odd Crystal Field

Let us now consider the electric dipole transitions caused by small odd crystal field with D_3 symmetry. The coordinate axes are taken as the z -axis is parallel to the C_3 axis and the y -axis is one of the C_2 axis. Then, the perturbing potential of symmetry D_3 of odd parity is given by

$$H_u = \sum_j V_u(r_j),$$

$$V_u(r_j) = Br_j^3 \left\{ -\frac{1}{\sqrt{2}} [Y_{33}(\theta_j, \phi_j) + Y_{3-3}(\theta_j, \phi_j)] \right\}, \quad (10)$$

where B' is a constant determined on the basis of a physical model, and H_u is the potential due to effective dipole moments located at the atoms attached to the metal ion.

Then B' is given as

$$B' = 6 \left(\frac{4\pi}{7} \right)^{3/2} e \frac{p+p'}{R^5}, \quad (11)$$

where p is the component of the dipole moment in the plane of bidentate ring and perpendicular to the direction of the metal-ligand bond, and p' is the component perpendicular to the plane

The matrix element of the electric dipole moment, which is allowed by small odd crystal field H_u , is given by

$$\langle 4i | \underline{m} | 4f \rangle = - \frac{2}{8E} \langle 4i | \underline{m} | H_u | 4f \rangle, \quad (12)$$

in the same approximation as in Eq.(8). The trigonal bases used in the calculation of matrix element $\langle 4i | \underline{m} | H_u | 4f \rangle$ are well summarized by Shinada¹⁸.

The numerical values of p and p' in Eq.(11) are approximated by μ , which is determined by the splitting of the 3d-level in a cubic field and by the value of $\langle r^4 \rangle_{Fe}$ obtained in the above section. Using the values, $\zeta = 400 \text{ cm}^{-1}$, $\delta E = 10^5 \text{ cm}^{-1}$ and $R = 4a_0$, we have calculated the electric dipole transition moments. The transition moments are calculated by the analogous formula as Eq.(7), and the oscillator strengths of the transitions are also calculated (Table IV). Using these results, the Faraday parameters A , B , and C are calculated, and the results are shown in Table V.

Table IV

Table V

IV. DISCUSSION

The absorption spectrum of $\text{Fe}(\text{C}_3\text{H}_2\text{O}_4)^{3-}$ exhibits two broad bands at lower energies, 900 nm and 640 nm, and a sharp band at 445 nm. Unfortunately we could not measure the MCD for the first band because of the limit of instrument. The higher energy transitions are masked by the onset of a high-intensity band. The observed MCD spectrum (Fig.1) shows $(\underline{B} + \underline{C}/kT)$ -term line shape at 640 nm. The MCD spectrum at 445 nm shows an interesting line shape, which gives us the information that two bands are overlapping. If we assume that the MCD comes from both \underline{A} -term and $(\underline{B} + \underline{C}/kT)$ -term of a transition, then we cannot understand the positive values of $[\theta]_M$ on both sides of a sharp and negative MCD band. We shall give the interpretation of these MCD band later in this section.

Let us now extract $(\underline{B} + \underline{C}/kT)$ by integrating the experimental MCD data according to Eq.(6). In order to estimate the order of magnitude for convenience, we shall tentatively resolve the MCD spectrum at 445 nm into two bands: one is a positive $(\underline{B} + \underline{C}/kT)$ -term line shape at slightly high frequency and another is a negative $(\underline{B} + \underline{C}/kT)$ -term line shape at slightly low frequency. The results are $(\underline{B} + \underline{C}/kT) = 7.39$ for the band at 640 nm, $(\underline{B} + \underline{C}/kT) = 2.92$ and $(\underline{B} + \underline{C}/kT) = -2.62$ for the lower and upper bands at 445 nm region, respectively (All values are in units of $10^{-24} \beta [\text{cm}^2] / [\text{cm}^{-1}]$).

To estimate theoretically the magnitude of \underline{A} -, \underline{B} -, and \underline{C} -terms in the region of the absorption band, the maximum contributions of each term to the MCD may be compared, of which the ratio is given by $3\sqrt{3}A/4\Gamma h : B : C/kT$. Let us assume $\Gamma \sim 2400 \text{ cm}^{-1}$ for the ${}^6A_{1g} \rightarrow {}^4T_{2g}(1)$ transition, $\Gamma \sim 800 \text{ cm}^{-1}$ for the ${}^6A_{1g} \rightarrow {}^4E_g(1)$, ${}^4A_{1g}$ transitions, and $kT = 200 \text{ cm}^{-1}$ (room temperature). First, we calculate the ratios for the transitions caused by odd crystal field. Thus the values of \underline{A} , \underline{B} , and \underline{C} presented in Table V are employed. The ratios are $-0.121 : 0.104 : 0.727$ for the ${}^6A_{1g} \rightarrow {}^4E_g(1)$ transition, $0.096 : -0.104 : -1.690$ for the ${}^6A_{1g} \rightarrow {}^4T_{2g}(1)$ transition, and the ${}^6A_{1g} \rightarrow {}^4A_{1g}$ transition is forbidden. The \underline{A} terms are small, which is in agreement with the observed MCD. However, the values of $(B + C/kT)$ are calculated to be 0 for ${}^6A_{1g} \rightarrow {}^4A_{1g}$, 0.831 for ${}^6A_{1g} \rightarrow {}^4E_g(1)$, and -1.794 for ${}^6A_{1g} \rightarrow {}^4T_{2g}(1)$, and these results contradict with the observed MCD.

Next, if we assume the transitions are caused by odd vibrations of $T_{1u}(\nu_3)$ mode, the \underline{A} , \underline{B} , and \underline{C} terms are in the ratio (See Table III) $0.175 : 0.342 : -1.048$ for the ${}^6A_{1g} \rightarrow {}^4A_{1g}$ transition, $-0.277 : -0.411 : 1.658$ for the ${}^6A_{1g} \rightarrow {}^4E_g(1)$ transition, and $-0.136 : 0.180 : 3.247$ for the ${}^6A_{1g} \rightarrow {}^4T_{2g}(1)$ transition. The \underline{A} terms are small, which is in agreement with the observed MCD, and this holds true also for the transition associated with the other odd vibrations of $T_{1u}(\nu_4)$ and $T_{2u}(\nu_6)$ modes. Further, the C/kT term is dominant in $(B + C/kT)$.

The calculated values of $(B + C/kT)$ for the ${}^6A_{1g} \rightarrow {}^4T_{2g}(1)$ transition are in good agreement with the observed MCD of the band at 640 nm. The calculated results show that the vibrations of T_{1u} mode are effective in promoting the ${}^6A_{1g} \rightarrow {}^4T_{2g}(1)$ transition. On the other hand, the calculated results for the ${}^6A_{1g} \rightarrow {}^4E_g(1)$ and ${}^6A_{1g} \rightarrow {}^4A_{1g}$ transitions show that the transitions caused by T_{1u} and T_{2u} modes of vibration give the comparable order of $(B + C/kT)$ values with opposite signs. Hatfield² observed the polarized crystal spectrum of $(NH_4)_3Fe(mal)_3$ and found two maxima: one at 22880 cm^{-1} and another at 22660 cm^{-1} . Assuming the splitting of the ${}^4A_{1g}$ and ${}^4E_g^{(0)}$ level to be 200 cm^{-1} (the transition ${}^6A_{1g} \rightarrow {}^4E_g(1) + h\nu_6$ at 22500 cm^{-1} and the transition ${}^6A_{1g} \rightarrow {}^4A_{1g} + h\nu_6$ at 22700 cm^{-1}), we have shown the magnitude of $(B + C/kT)$ by a diagram (Fig. 2) to see how the calculated results compose the MCD line shape. The qualitative feature of the observed MCD can be well explained by this diagram.¹⁹ On the other hand, if we assume that the ${}^4E_g^{(0)}$ level is higher than ${}^4A_{1g}$ level, we cannot understand the observed MCD. Therefore, we conclude that the ${}^4A_{1g}$ level is higher than ${}^4E_g^{(0)}$ level.

Fig. 2

Our MCD spectra are markedly similar to those of $Mn(H_2O)_6^{2+}$, which is isoelectronic with Fe^{3+} ion. The optical spectra of $Mn(H_2O)_6^{2+}$ are well characterized. If the first band of $Fe(C_3H_2O_4)_3^{3-}$ corresponds to the first band of manganese ion, i.e. to the ${}^6A_{1g} \rightarrow {}^4T_{1g}(1)$ transition, the MCD is expected to show the positive $[\theta]_M$ of $(B + C/kT)$ -term line shape. The calculated values of C/kT for the ${}^6A_{1g} \rightarrow {}^4T_{1g}(1)$ transition is found to be -3.961 , which is the same order of magnitude

with the value obtained for the ${}^6A_{1g} \rightarrow {}^4T_{2g}(1)$ transition and of opposite sign. Thus, the present studies on the MCD of ferric ion also support the previous assignment \checkmark : ${}^6A_{1g} \rightarrow {}^4T_{1g}(1)$ for the first band.

The oscillator strengths calculated as electric dipole transitions caused by odd crystal field (Table IV) are a little smaller than the observed ones, and the observed polarization data \checkmark cannot be explained well. In the present calculation of intensities of spin-forbidden bands, we have neglected the mixing of the higher 6Y states as in KP. On the other hand Holt and Dingle \checkmark have tried to explain the dichroism of trigonally distorted iron(III) complexes by including the mixing of higher 6Y states to 4f state, but the polarization behavior of absorption spectra could not be explained well.

The oscillator strengths calculated as electric dipole transitions caused by odd vibrations (Table II) are a little smaller than the observed ones, but the overall characters are in good agreement with experiment. The polarization behavior of the crystals of trigonally distorted ferric compounds cannot be well explained as an electric dipole transition caused by odd vibrations in an octahedral field, while the polarization behavior may be explained as the transitions which are allowed by vibrations in D_3 symmetry reduced from vibrations in O_h symmetry.

ACKNOWLEDGMENTS

The author is grateful to ^{Mr. H. Tomiyachi, Dr. T. Kato} Professors I. Tsujikawa, T. Murao and T. Yamamoto for their very valuable discussions and suggestions.

- 1 T.S.Piper and R.L.Carlin, J.Chem.Phys. 35, 1809 (1961).
- 2 W.E.Matfield, Inorg.Chem. 3, 605 (1964).
- 3 S.Holt and R.Dingle, Acta Chem.Scand. 22, 1091 (1968).
- 4 A.D.Duckingham and P.J.Stephens, Ann.Rev.Phys.Chem. 17, 399 (1966).
- 5 P.N.Schatz and A.J.McCaffery, Quart.Rev. 23, 552 (1969).
- 6 "Magneto Optical Effects" Symposia of the Faraday Society No 3 (1969) and references cited therein.
- 7 A.J.McCaffery, P.J.Stephens and P.N.Schatz, Inorg.Chem. 6, 1614 (1967).
- 8 P.J.Stephens, W.Suetaka and P.N.Schatz, J.Chem.Phys. 44, 4592 (1966).
- 9 P.J.Stephens. J.Chem.Phys. 52, 3489 (1970).
- 10 P.J.Stephens, R.L.Mowery and P.N.Schatz, J.Chem.Phys. 55, 224 (1971).
- 11 H.C.Clark, N.F.Curtis, and A.L.Odell, J.Chem.Soc. 1954, 63.
- 12 L.E.Orgel, J.Chem.Phys. 23, 1004 (1955).
- 13 Y.Tanabe and S.Sugano. J.Phys.Soc.Japan 9, 753, 766 (1954), ibid. 11, 864 (1956).
- 14 S.Koide and M.H.L.Pryce, Phil.Mag. 3, 607 (1958).
- 15 S.Koide, Phil.Mag. 4, 343 (1959).
- 16 E.Clementi, J.Chem.Phys. 41, 295 (1964).
- 17 Y.Tanabe, Progr.Theoret. Phys.(Kyoto) suppl. 14, 17 (1960).
- 18 M.Shinada, J.Phys.Soc.Japan 19, 1607 (1964).
- 19 The interpretation of the transitions ${}^4A_1 \rightarrow {}^4E_g$ and ${}^4A_1 \rightarrow {}^4A_1$ by H.Kato, M.Taniguchi and T.Kato [Chem. Phys. Letters 14, 231 (1972)] should be corrected as given here.

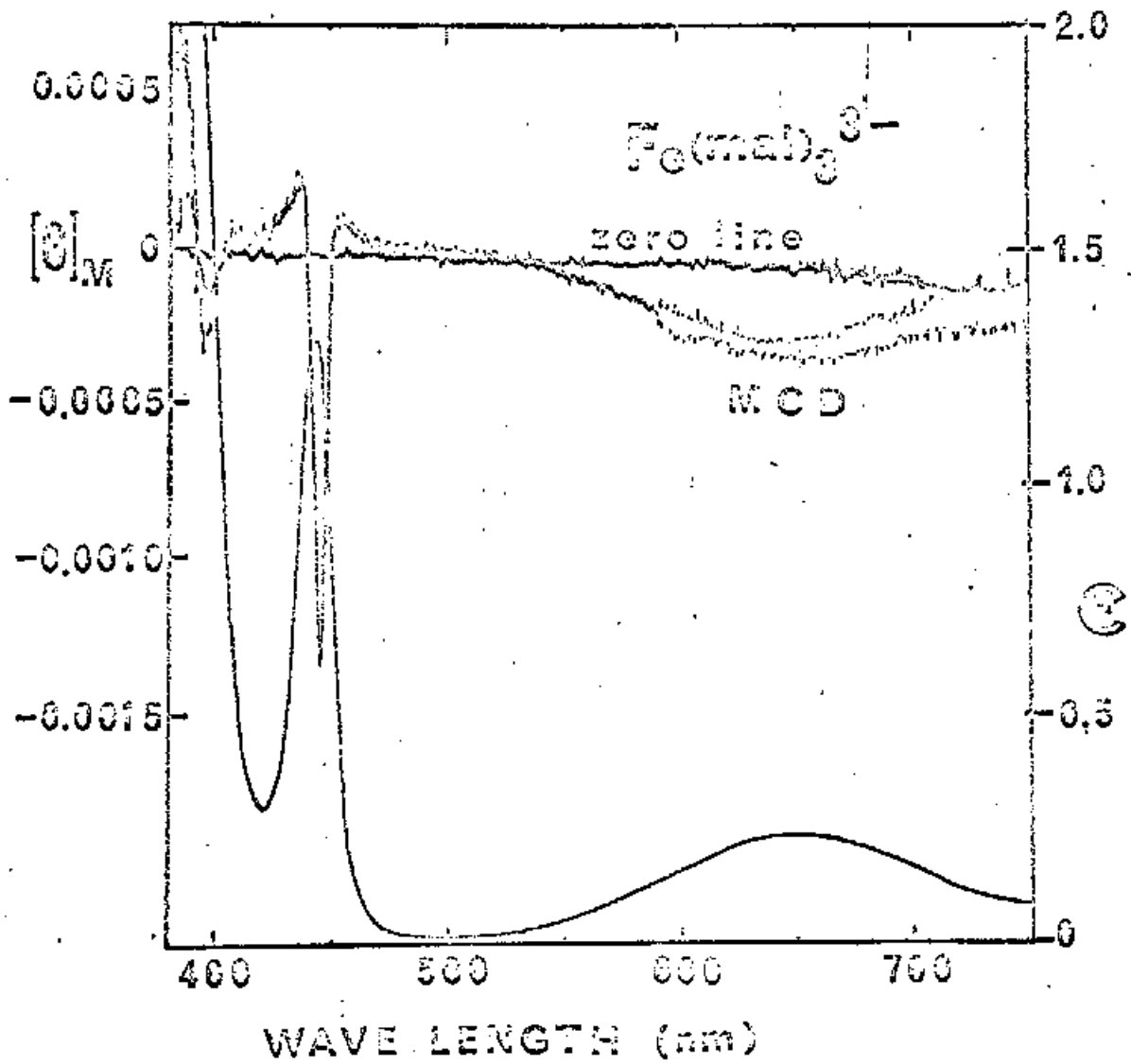


Fig.1. MCD and absorption spectrum of $Fe(C_2H_2O_4)_3^{3-}$ in water at room temperature (27±1°C). ϵ is the molar extinction coefficient. $[\theta]_M$ is the molar ellipticity per gauss.

Table I . States in the case of cubic field and the configuration, excitation energy from the ground state ${}^6A_{1g}$.

State	Energy (cm^{-1})	Configuration ^a
${}^6A_{1g}$	0	$d_{\underline{E}}^3({}^4A_2)dY^2({}^3A_2)$
${}^4A_{1g}$	22000	$d_{\underline{E}}^3({}^4A_2)dY^2({}^3A_2)$
${}^4A_{2g}$	35600	$d_{\underline{E}}^3({}^4A_2)dY^2({}^1A_1)$
${}^4E_g(1)$	22000	$\frac{2}{\sqrt{7}}d_{\underline{E}}^3({}^2E)dY^2({}^3A_2) + \frac{\sqrt{3}}{\sqrt{7}}d_{\underline{E}}^3({}^4A_2)dY^2({}^1E)$
${}^4E_g(2)$	26200	$\frac{\sqrt{3}}{\sqrt{7}}d_{\underline{E}}^3({}^2E)dY^2({}^3A_2) - \frac{2}{\sqrt{7}}d_{\underline{E}}^3({}^4A_2)dY^2({}^1E)$
${}^4T_{1g}(1)$	9650	$0.991d_{\underline{E}}^4({}^3F_1)dY + 0.094d_{\underline{E}}^3({}^2F_2)dY^2({}^3A_2) - 0.096d_{\underline{E}}^2({}^3F_1)dY^3$
${}^4T_{1g}(2)$	33000	$-0.055d_{\underline{E}}^4({}^3F_1)dY + 0.954d_{\underline{E}}^3({}^2F_2)dY^2({}^3A_2) - 0.354d_{\underline{E}}^2({}^3F_1)dY^3$
${}^4T_{1g}(3)$	41600	$0.123d_{\underline{E}}^4({}^3F_1)dY - 0.345d_{\underline{E}}^3({}^2F_2)dY^2({}^3A_2) + 0.930d_{\underline{E}}^2({}^3F_1)dY^3$
${}^4T_{2g}(1)$	13700	$0.969d_{\underline{E}}^4({}^3F_1)dY - 0.167d_{\underline{E}}^3({}^2F_2)dY^2({}^3A_2) - 0.181d_{\underline{E}}^2({}^3F_1)dY^3$
${}^4T_{2g}(2)$	24000	$0.174d_{\underline{E}}^4({}^3F_1)dY + 0.984d_{\underline{E}}^3({}^2F_2)dY^2({}^3A_2) + 0.022d_{\underline{E}}^2({}^3F_1)dY^3$
${}^4T_{2g}(3)$	46100	$0.175d_{\underline{E}}^4({}^3F_1)dY - 0.053d_{\underline{E}}^3({}^2F_2)dY^2({}^3A_2) + 0.983d_{\underline{E}}^2({}^3F_1)dY^3$

^a In cubic field the d -level split into two levels, i.e. the lower triply degenerate $d_{\underline{E}}$ of T_{2g} symmetry the upper doubly degenerate dY of E_g symmetry.

Table II. Oscillator strengths calculated as an electric dipole transition caused by odd vibrations.

Transition	Associated vibration	Oscillator strengths	
		Calculated.	Observed.
${}^6A_{1g} \rightarrow {}^4T_{2g}(1)$	$T_{1u}(\nu_3)$	$5.56 \cdot 10^{-7}$	$23 \cdot 10^{-7}$
	$T_{1u}(\nu_4)$	$3.44 \cdot 10^{-7}$	
	$T_{2u}(\nu_6)$	$0.47 \cdot 10^{-7}$	
${}^6A_{1g} \rightarrow {}^4E_g(1)$	$T_{1u}(\nu_3)$	$3.94 \cdot 10^{-7}$	} $52 \cdot 10^{-7}$
	$T_{1u}(\nu_4)$	$1.22 \cdot 10^{-7}$	
	$T_{2u}(\nu_6)$	$4.59 \cdot 10^{-7}$	
${}^6A_{1g} \rightarrow {}^4A_{1g}$	$T_{1u}(\nu_3)$	$2.69 \cdot 10^{-7}$	
	$T_{1u}(\nu_4)$	$0.89 \cdot 10^{-7}$	
	$T_{2u}(\nu_6)$	$2.95 \cdot 10^{-7}$	
${}^6A_{1g} \rightarrow {}^4T_{1g}(1)$	$T_{1u}(\nu_3)$	$1.52 \cdot 10^{-7}$	$11 \cdot 10^{-7}$
	$T_{1u}(\nu_4)$	$2.61 \cdot 10^{-7}$	
	$T_{2u}(\nu_6)$	$0.11 \cdot 10^{-7}$	

Table III. Faraday parameters A , B , and C calculated as an electric dipole transition caused by odd vibrations.

Transition	Associated vibration	Faraday parameter (Cal.)			$(\frac{B}{A} + \frac{C}{kT})^b$	
		A^a	B^a	C^a	Cal.	Obs.
${}^6A_{1g} \rightarrow {}^4T_{2g}(1)$	$T_{1u}(\nu_3)$	-251.5	0.180	649.4	3.427	7.59
	$T_{1u}(\nu_4)$	-42.1	0.039	148.1	0.780	
	$T_{2u}(\nu_6)$	6.8	0.040	-20.5	-0.063	
${}^6A_{1g} \rightarrow {}^4E_g(1)$	$T_{1u}(\nu_3)$	-170.6	-0.411	331.6	1.247	2.92
	$T_{1u}(\nu_4)$	-15.7	0.231	30.6	0.384	
	$T_{2u}(\nu_6)$	180.2	0.033	-350.3	-1.719	
${}^6A_{1g} \rightarrow {}^4A_{1g}$	$T_{1u}(\nu_3)$	107.8	0.342	-209.6	-0.706	-2.62
	$T_{1u}(\nu_4)$	35.2	-0.214	-68.4	-0.556	
	$T_{2u}(\nu_6)$	-118.8	0.057	231.0	1.212	

^a In units of $10^{-24} \beta e^2 [\text{cm}^2]$. ^b In units of $10^{-24} \beta e^2 [\text{cm}^2] / [\text{cm}^{-1}]$.

Table IV. Oscillator strengths calculated as an electric dipole transition caused by odd crystal field.

Transition	Polarization	Oscillator strengths
${}^6A_{1g} \rightarrow {}^4T_{2g}(1) : \rightarrow {}^4E$	σ	$3.47 \cdot 10^{-7}$
$\phantom{{}^6A_{1g} \rightarrow {}^4T_{2g}(1)} : \rightarrow {}^4A_1$	forbidden	0.0
${}^6A_{1g} \rightarrow {}^4E_g(1) : \rightarrow {}^4E$	σ	$3.75 \cdot 10^{-7}$
${}^6A_{1g} \rightarrow {}^4A_{1g} : \rightarrow {}^4A_1$	forbidden	0.0
${}^6A_{1g} \rightarrow {}^4T_{1g}(1) : \rightarrow {}^4E$	σ	$4.49 \cdot 10^{-7}$
$\phantom{{}^6A_{1g} \rightarrow {}^4T_{1g}(1)} : \rightarrow {}^4A_2$	π	$2.24 \cdot 10^{-7}$

Table V. Faraday parameters A , B , and C calculated as electric dipole transitions caused by odd crystal field.

Transition	Faraday parameter (Cal.)				
	D_3	A^C	E^C	C^C	$(B + C/kT)^b$
${}^6A_{1g} \rightarrow {}^4T_{2g}(1) : \rightarrow {}^4E$		176.5	-0.104	-338.0	-1.794
$\phantom{{}^6A_{1g} \rightarrow {}^4T_{2g}(1)} : \rightarrow {}^4A_1$		0	0	0	0
${}^6A_{1g} \rightarrow {}^4E_g(1) : \rightarrow {}^4E$		-74.8	0.104	145.4	0.831
${}^6A_{1g} \rightarrow {}^4A_{1g} : \rightarrow {}^4A_1$		0	0	0	0

^aIn units of $10^{-24} \text{pe}^2 [\text{cm}^2]$. ^bIn units of $10^{-24} \text{pe}^2 [\text{cm}^2] / [\text{cm}^{-1}]$.

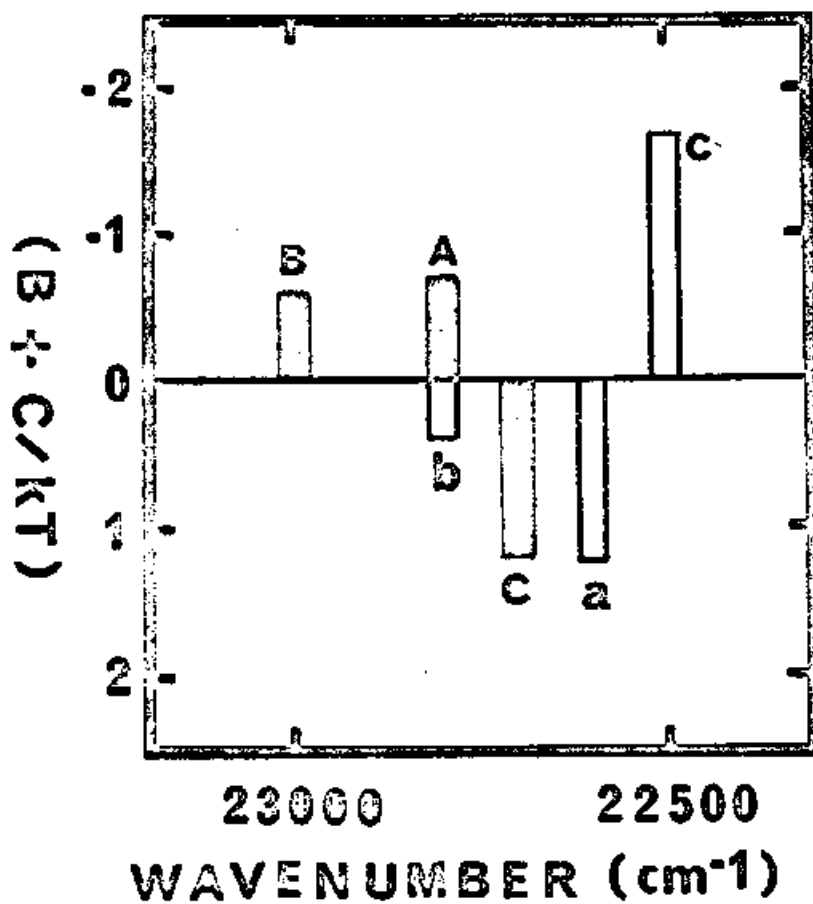


Fig. 2. A diagram shows how the calculated results compose the MCD line shape. a: transition ${}^6A_{1g} \rightarrow {}^4E_g(1) + h\nu_3$, b: transition ${}^6A_{1g} \rightarrow {}^4E_g(1) + h\nu_4$, c: transition ${}^6A_{1g} \rightarrow {}^4E_g(1) + h\nu_6$, A: transition ${}^6A_{1g} \rightarrow {}^4A_{1g} + h\nu_3$, B: transition ${}^6A_{1g} \rightarrow {}^4A_{1g} + h\nu_4$, C: transition ${}^6A_{1g} \rightarrow {}^4A_{1g} + h\nu_6$.